Ecotoxicology and Human Environmental Health

Next-generation complex metal oxide nanomaterials negatively impact growth and development in the benthic invertebrate Chironomus riparius upon settling

Nicholas Niemuth, Becky Curtis, Mimi Ngoc Hang, Miranda J. Gallagher, D. Howard Fairbrother, Robert J Hamers, and Rebecca D. Klaper

Environ. Sci. Technol., **Just Accepted Manuscript** • DOI: 10.1021/acs.est.8b06804 • Publication Date (Web): 15 Mar 2019

Title: Next-generation complex metal oxide nanomaterials negatively impact growth and development in the benthic invertebrate *Chironomus riparius* upon settling

Nicholas J. Niemuth[1], Becky J. Curtis[1], Mimi N. Hang[2], Miranda J. Gallagher[3], D. Howard Fairbrother[3], Robert J. Hamers[2], Rebecca D. Klaper[1]*

[1] School of Freshwater Sciences, University of Wisconsin-Milwaukee, 600 E Greenfield Ave., Milwaukee, WI 53204

[2]Department of Chemistry, University of Wisconsin-Madison, 1101 University Ave., Madison, WI 53706

[3]Department of Chemistry, Johns Hopkins University, 3400 North Charles St., Baltimore, MD 21218

*Corresponding Author

rklaper@uwm.edu, Phone: 414-382-1713, Fax: 414-382-1705

Abstract

Most studies of nanomaterial environmental impacts have focused on relatively simple first-generation nanomaterials, including metals or metal oxides (e.g. Ag, ZnO) for which dissolution largely accounts for toxicity. Few studies have considered nanomaterials with more complex compositions, such as complex metal oxides, which represent an emerging class of next-generation nanomaterials used in commercial products at large scales. In addition, many nanomaterials are not colloidally stable in aqueous environments and will aggregate and settle, yet most studies use pelagic rather than benthic-dwelling organisms. Here we show that lithium cobalt oxide ($Li_xCo_{1-x}O_2$, LCO) and lithium nickel manganese cobalt oxide ($Li_xNi_yMn_zCo_{1-y-z}O_2$, NMC) exposure of the model benthic species *Chironomus riparius* at 10 and 100 mg·L^{-1} caused 30-60% declines in larval growth, and a delay of 7-25 d in adult emergence. A correlated 41-48% decline in larval hemoglobin concentration and related gene expression changes suggest a potential adverse outcome pathway. Metal ions released from nanoparticles do not cause equivalent impacts, indicating a nano-specific effect. Nanomaterials settled within 2 days and indicate higher cumulative exposures to sediment organisms than those in the water column, making this a potentially realistic environmental exposure. Differences in toxicity between NMC and LCO indicate compositional tuning may reduce material impact.

TOC Art

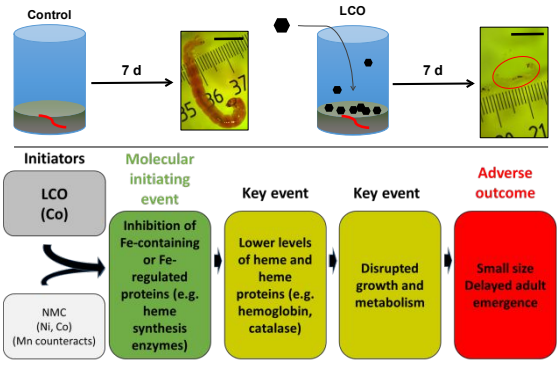

Introduction

Standard aquatic toxicity assays using pelagic organisms (e.g *Daphnia magna*, *Danio rerio*) have demonstrated a range of potential environmental impacts depending on the types of engineered nanomaterials (ENMs) considered, with some being toxic at low concentrations when considered over a chronic exposure but many not toxic until very high unrealistic concentrations.[1] However, most pristine ENMs are not stable in aqueous exposure conditions,[2] and thus many studies on pelagic organisms largely assume exposure to the stable fraction of ENMs left behind in the water column after a majority settles out.[2,3] Testing for impacts of ENMs on benthic organisms is therefore extremely important, in certain cases perhaps more important than impacts on pelagic organisms, as many ENMs are expected to settle and concentrate to higher exposure concentrations in sediment.[3,4] Despite this, the preponderance of aquatic nanotoxicology research has focused on exposures to pelagic organisms.[3]

Most ENM toxicity studies have also focused on first-generation materials, including metal nanoparticles, Au and Ag, and metal oxide nanoparticles, TiO_2, ZnO, and CeO_2,[5] as they have demonstrated potential for the highest use. For these materials, dissolution is often identified as the main source of toxicity.[6] However, we have comparatively little information on more complex next-generation ENMs that are now coming to use in the marketplace. The complex metal oxides lithium cobalt oxide ($Li_xCo_{1-x}O_2$, LCO) and lithium nickel manganese cobalt oxide ($Li_xNi_yMn_zCo_{1-y-z}O_2$, NMC) and other related complex metal oxides are examples of next-generation materials that are increasing dramatically in the marketplace due to their use as electrode materials in lithium ion batteries (LIBs)[7–10] and lower-volume applications such as catalysts for solar fuel production.[11] NMC is an alternative to LCO that has the same crystal

structure, but partial substitution of Co with Ni and Mn lowers cost and can increase performance.[12] A typical electric vehicle contains approximately 35-90 kg of metal oxide particles, with rapid increases in electric vehicle production leading to predicted global production of 300-800 kilotons of Co and Ni annually by 2025,[13]and LIB waste by 2025 estimated to reach 200 kilotons from EVs alone.[14] Present-generation batteries frequently use particle sizes in the micron range, but smaller particles in the nanometer size regime achieve fast recharge times and are also formed *in situ* by mechanical fracturing of larger particles during use.[12] Because lithium-ion batteries are not generally recycled due to the low cost of Ni and Mn,[13,15] potential release of cathode materials in micron- and nano-particle form into the aquatic environment from battery waste is a legitimate concern.[16,17]

Previous research has demonstrated that the complex metal oxides NMC and LCO do not behave or cause toxicity in the same manner as their simple metal oxide counterparts.[18,19] For example, density functional calculations and experimental measurements showed that NMC dissolves incongruently, with Ni released more rapidly in aqueous media compared with Co and Mn.[18] Material dissolution is also impacted by properties of the media such as pH.[18] A consequence of incongruent dissolution is that the ions released and ENM composition change over the course of the exposure. Ni and Co are both toxic to pelagic and benthic organisms,[20–23] while Mn is relatively non-toxic.[24,25] Our previous study showed that concentrations of LCO and NMC as low as 0.25 $mg \cdot L^{-1}$ have significant negative impacts on survival and reproduction in *Daphnia magna* that are not accounted for by particle dissolution.[19] This work also showed that NMC exposure produced lower daphnid toxicity compared to LCO, indicating a difference due to ENM composition[19]

Metal oxide nanoparticles including TiO_2, ZnO, and CeO_2 have been shown to settle over time in aqueous media at ambient pH.[26–28] We previously showed both LCO and NMC nanoparticles settle substantially within 24 hours in aqueous media: 66 and 33% settling in 22.5 h respectively.[19] Thus, testing for impacts of these materials on benthic organisms is warranted.

For this study, impacts of ENMs entering the environment were investigated using freshwater midge *Chironomus riparius*, a model species for testing effects of chemical exposures on benthic organisms. This organism is a keystone species and an important food source in both aquatic and terrestrial environments.[29] It has been shown to be sensitive to pollutants, and protocols for exposure and culturing have been established by the American Society for Testing and Materials and U.S. Environmental Protection Agency.[30] The *C. riparius* genome is sequenced,[31] and large mRNA and expressed sequence tag (EST) databases exist for *C. riparius*, including genes relevant to stress and the response to chemical exposures. *C. riparius* have also been used rarely but successfully in ENM toxicity exposures,[32–36] though only one study (of fullerene ENMs) has explicitly looked at impacts of material settling.[34] In the current study, *C. riparius* larvae were exposed to LCO and NMC at 1, 10, and 100 $mg \cdot L^{-1}$ as well as ion controls from 5 days post-hatch until adult emergence and organisms were evaluated for changes in size, coloration, and gene expression at 7 d and adult emergence up to 50 d. Results indicate significant negative impacts on all of these endpoints from LCO and NMC exposure, which are not replicated by ion controls. Implications of these effects in the context of the expected volume of LIB waste and settling of these materials in the environment are discussed, with compositional tuning indicated as a potential means of mitigating environmental impacts. This study demonstrates the

importance of using sediment species for testing environmental impacts, reveals,a nano-specific impact of complex nanoparticles, and indicates a potential adverse outcome pathway for metal oxide NPs.

Materials and methods

Synthesis of LCO and NMC nanosheets

Synthesis of LCO and NMC nanosheets was carried out using methods described in [37,38] and consists of two steps. All reagents used for synthesis were purchased from Sigma Aldrich and only ultrapure water was used. To specifically make LCO nanosheets, cobalt hydroxide nanosheets were first synthesized using a precipitation method where in 1 M cobalt (II) nitrate was added dropwise into a 0.1 M LiOH solution under magnetic stirring. The resulting precipitate was then cleaned using repeated cycles (3X) of centrifugation and resuspension in ultrapure water (18 M**Ω** cm resistivity) followed by repeated cycles (2X) of centrifugation and resuspension in methanol. The precipitate (200 mg) was then dried under a continual flow of nitrogen gas and subsequently was added to a 10 g mixture of molten lithium salt consisting of a molar ratio of 6:4 LiOH: $LiNO_3$ (205 °C, under magnetic stirring) in a poly(tetrafluorethylene) vessel. After 1 h, the reaction was carefully quenched with ultrapure water and the LCO precipitate was purified using repeated cycles of centrifugation and resuspension in ultrapure water (2X) and methanol (3X) before drying under a flow of nitrogen gas. All centrifugation was completed using the Thermo Scientific Sorvall Legend X1R Centrifuge with a Thermo TX-400 rotor at 4696 g. To synthesize NMC nanosheet, an identical method was used with the exception that in the precipitation step, a ratio of 1:1:1 of Ni:Co:Mn salts (0.1 M nickel (II) acetate, 0.1 M

cobalt (II) acetate, and 0.1 M manganese (II) acetate) were used instead. The degree of lithiation was not directly controlled for using this synthetic method. Characterization of nanosheet stoichiometry, crystal phase, and size and morphology from XRD, ICP-OES and SEM are included in the Supporting Information.

C. riparius larval exposure

ENM stock suspension

Stock solutions of LCO and NMC (200 $mg \cdot L^{-1}$) were prepared by adding 40 mg of ENM powder to 200 mL of Milli-Q® water and sonicating at 100% power for 20 minutes in a Branson 2800 ultrasonic bath (Emerson Electric Co, St Louis, MO). Dilutions to 20 and 2 $mg \cdot L^{-1}$ were made in Milli-Q® and sonicated for an additional 10 min immediately before dosing. Zeta potential of ENMs at final concentrations in 1x Moderately Hard Reconstituted Water (MHRW)[19] were characterized using a Zetasizer Nano ZS (Malvern Instruments, Westborough, MA, USA).

Exposure beaker preparation and maintenance

Exposure beakers were prepared by adding 15 g of 140-270 mesh silica sand (AGSCO Corp) to 100 mL beakers and autoclaving to sterilize. Sand was then rinsed 3x with 80 mL Milli-Q®. Control beakers were prepared by adding 20 mL of Milli-Q® and 20 mL of 2x MHRW. Treatment beakers (1, 10, and 100 $mg \cdot L^{-1}$) were prepared by adding 20 mL of 2x MHRW and 20 mL of the appropriate 2x nanoparticle stock. Five *C. riparius* larvae (5 days post-hatch) were added to each replicate control and exposure beaker.

Beakers were covered with plastic wrap and incubated at 20 °C with a 16:8 light:dark photoperiod. A 50% water exchange was carried out three times per week. For exposure beakers, new ENMs were not added, as ENMs had settled by this time. Animals were fed ground TetraMin® flakes (20 $g \cdot L^{-1}$ in Milli-Q®) daily, 125 uL per beaker.

ENM exposures

An initial LCO exposure was conducted with 10 replicate beakers per condition (5 larvae per beaker) each for control, 1, 10 and 100 $mg \cdot L^{-1}$. A second round of experiments was carried out with 10 replicate beakers per condition to compare LCO to NMC, exposing larvae to LCO at 1, 10, and 100 $mg \cdot L^{-1}$; NMC at 1, 10, and 100 $mg \cdot L^{-1}$; and control. For both sets of experiments, larvae were harvested from 5 beakers per condition on exposure day 7 and frozen for gene expression analysis. The remaining 5 beakers per condition were maintained until exposure day 50 for adult fly emergence.

Having observed changes in size and coloration of ENM-exposed larvae, a third experiment was conducted with 5 replicate beakers per condition, exposing larvae to LCO at 1, 10, and 100 $mg \cdot L^{-1}$; NMC at 1, 10, and 100 $mg \cdot L^{-1}$; and control. Larvae from all 5 beakers were harvested on exposure day 7, flash frozen in liquid nitrogen, and stored at – 80 °C for imaging for size and coloration analysis.

Ion control exposures

Data from ICP-MS analysis (see *ICP-MS analysis of released ions* below) were used to determine the concentrations for 2x stocks of metal salts to yield exposure concentrations

reflective of ion concentrations found in the supernatants of 10 and 100 mg·L^{-1} LCO and NMC exposure media samples. We chose to test whether the ions observed released from the particles were by themselves sufficient to cause any observed toxicity, as metal dissolution from NPs is indicated as a major cause of toxicity in other studies. If not, then the portion of settled particles, by concentrating material in the sand, are the cause of toxicity: either by direct nano-toxic effects of the particles themselves or by acting as a vector to bring particles with high concentrations of metals into the feeding environment of the larvae. Animals were dosed with Li, Ni, Mn, and Co ions at the highest concentration observed over 7 d. For LCO, dosed ions were 1000 µg·L^{-1} Li and 400 µg·L^{-1} Co for 10 mg·L^{-1} and 4200 µg·L^{-1} Li and 900 µg·L^{-1} Co for 100 mg·L^{-1}. For NMC, dosed ions were 710 µg·L^{-1} Li, 360 µg·L^{-1} Ni, 270 µg·L^{-1} Mn, and 160 µg·L^{-1} Co for 10 mg·L^{-1} and 7000 µg·L^{-1} Li, 2000 µg·L^{-1} Ni, 300 µg·L^{-1} Mn, and 600 µg·L^{-1} Co for 100 mg·L^{-1}. An ion control exposure was conducted with 10 replicate beakers per condition: control, LCO 10 and 100 mg·L^{-1} ion equivalents, and NMC 10 and 100 mg·L^{-1} ion equivalents. At water changes, 20 mL of exposure media was removed and replaced with 20 mL of 1x ion solution to maintain ion concentrations throughout the exposure. Larvae were harvested from 6 beakers per condition on exposure day 7: 3 beakers per condition for gene expression analysis were frozen and 3 beakers per condition for imaging and size measurement were preserved in 70% ethanol. The remaining 4 beakers per condition were maintained until exposure day 50 for adult fly emergence.

ICP-MS analysis of released ions

Inductively coupled plasma mass spectrometry (ICP-MS) was conducted on exposure media at all concentrations to determine the level of metal dissolution into exposure media after 2, 4, and

7 d, sampling exposure beakers before each water change over the first seven days of the experiment. Supernatant of centrifuged samples were acidified to 2% wt nitric acid and analyzed with an Elan DRC II ICP-MS (Perkin Elmer). 10 to 150-fold dilutions were carried out on supernatants containing ions at concentrations above 100 ppb to ensure analyte concentrations fell within the detection range of the instrument. The calibration curve was prepared from serial dilutions of 1003 ± 5ppb Ni, 1007 ± 4ppb Mn, 996 ± 3ppb Co, and 1006 ± 2ppb Li NIST Traceable standards (Inorganic Ventures). Full details for sampling and quantification are included in the Supporting Information.

ENM sedimentation behavior

We previously showed that LCO and NMC settle out in MHRW.[19] To determine the extent of particle settling in this study, we sampled exposure treatments of 1, 10, and 100 $mg \cdot L^{-1}$ of LCO or NMC particles in 1x MHRW on exposure days 0, 2, 4, and 7. Absorbance values of sampled supernatants were measured at 600 nm using a Synergy H4 plate reader (Biotek Instruments, Winooski, VT).

Imaging and measurement

Size

Flash frozen and alcohol-preserved larvae were imaged using a Motic SMZ-168 TL stereomicroscope with an attached Moticam 2, 2.0 MP CMOS camera (Motic, Hong Kong). Images were recorded using Motic Images Plus 2.0 software, and the included measurement tool used to determine animal size metrics. Measurements were calibrated with a Leica 50 mm metric stage micrometer (Leica Camera AG, Wetzlar, Germany).

220

221 *Animal coloration (Hemoglobin absorbance)*

222 The green channel from an RGB (red-green-blue) image was isolated and pixel intensity used to
223 measure the absorbance of hemoglobin (Hb) in *C. riparius* larvae on day 7. Hb absorbance
224 analysis was only carried out on flash-frozen larvae, as those preserved in ethanol did not retain
225 intact Hb. Detailed information on image processing is included in the Supporting Information.

226

227 ***Gene expression analysis***

228 Total RNA was extracted from flash-frozen 7 d exposure samples and 100 ng of total RNA
229 transcribed into complementary deoxyribonucleic acid (cDNA). Gene expression analysis was
230 carried out on a variety of genes associated with metal, oxidative, protein, and general stress
231 responses. The following were analyzed for gene expression: ribosomal protein *RPL13*
232 (housekeeping gene); metal stress gene metallothionein (*MTT*), as metal exposure is
233 hypothesized to be a major source of toxicity; oxidative stress genes: catalase (*CAT*), gamma-
234 glutamylcystein synthase (*GCS*), glutathione s-transferase (*GST*), and two different superoxide
235 dismutases (*Cu-ZnSOD* and *MnSOD*), as oxidative stress is hypothesized to be a main cause of
236 damage by nanoparticle exposures; heat shock protein *HSP27*, important for protecting protein
237 folding after exposure to toxins; stress-responsive regulatory kinase *p38*; developmental
238 regulator ecdysone receptor (*EcR*), to measure changes in developmental pathways as a result of
239 exposure; and genes related to heme synthesis, added as we found an indication in the change of
240 heme production in exposed organisms: aminolevulinic acid synthase (*ALAS*), porphobilinogen
241 synthase (*PBGS*), and heme oxygenase (*HO)* (Table S1).

242

Relative gene expression was quantified using the iTaq Universal SYBR Green Supermix (Bio-Rad, Hercules, CA) for 20 μL reactions and the $2^{-\Delta\Delta Ct}$ method.[39] For detailed information on extraction, cDNA creation, primer design, and qPCR, see the Supporting Methods.

Statistical analysis

Statistical analyses were performed using SPSS version 22 for Mac (IBM). Statistical tests for each dataset were chosen based on data normality determined by the Shapiro-Wilk test and equality of variance using Levene's test. Normally distributed data with equal variance (width, Hb concentration) were compared using a one-way ANOVA with Tukey post-hoc comparisons. Data with normal distributions but unequal variances (gene expression) were compared using a Welch one-way ANOVA with Dennett's T3 post-hoc comparisons. Non-normal data were compared using Kruskal-Wallis (length, head capsule length) or Kaplan-Meier (time to emergence) non-parametric tests. Significance for all statistics was set at $p < 0.05$. Datasets with a nested design (size, Hb, emergence) were tested for any replicate effect; no replicate effects were detected for any dataset ($p > 0.05$).

Results and Discussion

Our results show that next-generation complex metal oxide ENMs LCO and NMC settle in aqueous media and cause significant, negative, nano-specific effects on the keystone benthic species *C. riparius*, impacting their size, time to emergence, Hb levels, and expression of stress and heme-metabolism genes. Impacts of these ENMs are nano-specific, as the effects of ENM exposure exceed or are absent in equivalent ion exposures. Effects are much greater for LCO than the alternative NMC materials providing an indication that using NMC may cause less

environmental impact. Impacts on Hb levels and gene expression may point to the molecular mechanism underlying these effects in chironomids.

LCO and NMC aggregate and settle

LCO and NMC both settled substantially over the course of the experiment: more than 90% of material within 2 d for 100 $mg \cdot L^{-1}$ exposures, and more than 70% of material within 2 d at 10 $mg \cdot L^{-1}$ (Fig S3). Settling is more rapid for higher concentrations, as has been observed for other ENMs including CeO_2, TiO_2, and iron oxides.[40–42] Zeta-potential data point to an explanation for this concentration-dependent settling. Zeta-potential values for LCO and NMC at their moment of addition are highly negatively charged in 1 $mg \cdot L^{-1}$ exposures (-16.33 and -17.73 mV respectively), while 10 $mg \cdot L^{-1}$ exposures are slightly less negative (-7.74 and -6.07 mV), and values approach neutral to slightly positive at 100 $mg \cdot L^{-1}$ (0.52 and 1.59 mV) (Table S2). Electrostatic repulsion is one of the primary sources of ENM stability in aqueous media.[43] Thus, increased settling at higher LCO and NMC exposure concentrations is likely due to an increased propensity for particles to aggregate due to lower electrostatic repulsion.

Aggregation of LCO and NMC at higher concentrations likely underlies observed concentration-dependent declines in material dissolution. For both materials all intercalated Li left the material by the 2 d time point, but even at high concentrations lithium is not considered toxic to these organisms (Fig S4d).[19] For LCO, ICP-MS results showed that dissolution of Co ions from the material did not scale linearly with exposure concentration, but rather proportionally to the $\log_{10}$ of the exposure concentration. That is, dissolved Co for 100 $mg \cdot L^{-1}$ LCO was only 2-3x the dissolved Co for 10 $mg \cdot L^{-1}$, which was only 2-3x the dissolved Co for 1 $mg \cdot L^{-1}$, rather than the

289 10x that might be expected (Fig S4c). Only a portion of Co from the material dissolved over the
290 course of 7 d, although relatively more Co dissolved as ions at 1 $mg \cdot L^{-1}$ (39%) than at 10 $mg \cdot L^{-1}$
291 (14%) or 100 $mg \cdot L^{-1}$ (5%) (Fig S5c). For NMC particles, ICP-MS results indicated dissolution of
292 Ni, Mn, and Co from the material over the course of 7 d, with most dissolution for these metals
293 occurring by day 2 for 1 and 10 $mg \cdot L^{-1}$ exposures (Fig S4). Dissolved ion concentration for Ni,
294 Mn, and Co was proportional to the $\log_{10}$ of exposure concentration over 7 d, similar to Co for
295 LCO (Fig S4). Only a fraction of Ni, Mn, or Co dissolved from the material over 7 d, with
296 relatively more metal dissolving as ions at lower exposure concentrations: 1 $mg \cdot L^{-1}$ – 67% of Ni,
297 55% of Mn, and 49% of Co; 10 $mg \cdot L^{-1}$ - 30, 24, and 25% respectively; 100 $mg \cdot L^{-1}$ – 9, 6, and
298 12% respectively (Fig S5).
299
300 Thus, more metal as a percent of total material mass dissolved at lower concentrations than at
301 higher concentrations: about 50% at 1 $mg \cdot L^{-1}$, about 25% at 10 $mg \cdot L^{-1}$, and only about 10% at
302 100 $mg \cdot L^{-1}$ (Fig S5). The lower surface-area-to-volume ratio of aggregated particles formed at
303 high concentrations likely reduces ion dissolution from the material, as has been shown for NMC
304 with different surface-area-to-volume ratios.[12] Since only a small percentage of ions dissolve
305 from the material, particularly at higher concentrations, particle exposures, by concentrating
306 large amounts of settled material in surface sand, have impacts of a much higher degree than —
307 or are unobservable in — ion exposures.
308
309 ***LCO and NMC impact* C. riparius *growth and adult emergence***
310 Particle exposure causes significant, dose-dependent effects on the development of *C. riparius*
311 larvae not explicable by ion dissolution into the media, retarding growth and delaying emergence

of adult flies. Larvae in exposures were 30% (LCO and NMC 10 $mg \cdot L^{-1}$) to 60% (100 $mg \cdot L^{-1}$ LCO) smaller than controls (Fig 1a, c, and e; e.g. lengths of 3.2 ± 0.8 mm for LCO 10 $mg \cdot L^{-1}$ and 1.8 ± 0.2 mm for LCO 100 $mg \cdot L^{-1}$ versus 4.5 ± 0.2 mm for control). Ion exposures only caused a 20% decrease in size and at the highest concentration, representative of 100 $mg \cdot L^{-1}$ NMC (Fig 1b and d). Emergence was also significantly delayed for particle-exposed animals at 10 and 100 $mg \cdot L^{-1}$ for LCO and at 100 $mg \cdot L^{-1}$ for NMC (Fig 2a). Ion exposures showed no impact on emergence (Fig 2b), demonstrating the importance of settled nanomaterials for these impacts. Toxicity of Ni to *C. riparius* has been fairly well studied in the literature. Accounting for the amount of Co and Ni in added LCO and NMC, impacts on *C. riparius* larval growth were seen at concentrations 10-30 fold lower than that seen in the literature for Ni-spiked sediment: 11-16 $mg \cdot kg^{-1}$ for 10 $mg \cdot L^{-1}$ NMC and LCO, respectively, versus 146-358 $mg \cdot kg^{-1}$ in Ni-spiked sediment.[21,44] No impacts were seen on emergence from Ni-spiked sediments even up to 7990 $mg \cdot kg^{-1}$,[21] whereas impacts were observed from LCO at 16 $mg \cdot kg^{-1}$ (10 $mg \cdot L^{-1}$ exposure) and NMC at 112 mg kg^{-1} (100 $mg \cdot L^{-1}$ exposure). Thus, toxicity from settled ENM exceeds that expected from sediment-spiked ions based on the literature. The concentration of metal particles at the sediment surface and *C. riparius* feeding behavior may account for increased toxicity from ENMs, as discussed below.

Metal-specific differences in ENM toxicity

Importantly, LCO 10 $mg \cdot L^{-1}$ exposures caused a significant delay in emergence at a concentration an order of magnitude lower than seen in NMC (100 $mg \cdot L^{-1}$). Larvae from 100 $mg \cdot L^{-1}$ LCO exposures did not emerge even up to exposure day 50, more than double the emergence time of controls, despite being visible in disturbed sand.

335

336 Differences in response between NMC and LCO may be related to compositional differences
337 between the two ENMs. While the amount of settled material was similar for both materials, not
338 all metals in these materials are expected to elicit the same toxicity. Ni and Co are both toxic
339 metals. On a per mass basis, LCO has 50% more toxic metal than NMC, as it contains only
340 cobalt, while NMC includes Mn in addition to Ni. Cobalt has been shown to cause oxidative
341 stress by depleting reduced thiols from cells.[45] Nickel is also known to cause oxidative stress,[46]
342 and may cause oxidative damage that would elicit a response similar to Co. Both Co_3O_4 and NiO
343 ENMs have been shown to cause oxidative stress *in vitro*.[47,48] Manganese, however, has been
344 shown to have antioxidant properties in rats, counteracting the oxidative impacts of other heavy
345 metals,[49] and MnO_2 ENMs have been shown to scavenge ROS *in vitro*.[50]

346

347 Differing gene expression patterns between LCO and NMC may be related to these
348 compositional differences. *MTT* gene expression, related to metal ion exposure and toxicity,
349 declined significantly and in a dose-dependent manner with increasing LCO exposure while
350 NMC had no impact on its expression (Fig 3c). For *CAT* and *HSP27*, 1 $mg \cdot L^{-1}$ NMC had the
351 opposite effect of LCO at 100 $mg \cdot L^{-1}$, with expression moving in parallel as dose increased (Fig
352 3a and b). Manganese has been shown to decrease expression of *EcR* in the amphipod *T.*
353 *japonicas,*[51] which may explain reduced *EcR* expression in NMC-exposed larvae (Fig 3d). The
354 antioxidant properties of Mn, and the overwhelming of this antioxidant effect with increasing Co
355 and Ni, may explain observed gene expression patterns and account for the lower observed
356 impact of NMC compared to LCO in this study and in our previous work.[19] Thus, tuning of
357 material composition may be a means of mitigating material impact.

Impact of cobalt on heme synthesis as a potential mechanism of toxicity and adverse outcome pathway

Larvae exposed to LCO and NMC showed significantly reduced levels of Hb beginning at 10 $mg \cdot L^{-1}$ exposure (Fig 1g). This paralleled cobalt disruption of heme synthesis enzymes observed in other organism such as avian and rat liver cells.[52,53] Bacterial and animal studies suggest that the mechanism of cobalt interference with heme biosynthesis is perhaps through substituting cobalt for iron.[54]

Increased expression of *ALAS* and decreased expression of *PBGS* observed in this study (Figs 3e and f) are indicative of inhibition of heme synthesis by Co.[52] *ALAS* expression was up significantly at NMC 100 $mg \cdot L^{-1}$ (Fig 3e). *PBGS* expression appeared to decline with dose, particularly for LCO exposure, being significantly down-regulated for both LCO and NMC at 100 $mg \cdot L^{-1}$ (Fig 3f). Dose-dependent reductions in expression of *CAT*, an oxidative stress gene that requires heme, in LCO-exposed larvae at 10 and 100 $mg \cdot L^{-1}$ (Fig 3a) may also point to disruption of heme synthesis by Co as a mechanism of toxicity. Cobalt exposure has been shown to have a strong negative impact on catalase expression in liver of rats[55] and goldfish.[56]

Both Hb levels and *PBGS* expression correlated inversely with the $\log_{10}$ of Co settled in LCO and NMC (Hb: $R^2 = 0.848$, $\beta = -2.25$, $p < 0.001$; *PBGS*: $R^2 = 0.681$, $\beta = -0.314$, $p < 0.05$). Inhibition of Hb in *Tanytarsus* chironomids by carbon-monoxide was previously shown to reduce chironomid metabolism and increase larval mortality.[57] The importance of functional Hb for normal chironomid metabolism thus suggests that inhibition of heme synthesis by cobalt may

underlie the developmental impacts of LCO and NMC exposure. A proposed adverse outcome pathway summarizing this is presented in Fig 4.

Benthic organisms are susceptible to settled ENMs

Settling in aqueous environments is characteristic of many ENMs.[2,58] This settling will cause their accumulation in the sediment and an increase in accumulation over time with continual introduction, which may impact benthic organisms. ENMs in sediment could have a particular impact on deposit feeders that uptake sediment particles like *C. riparius* larvae, which feed primarily on detritus < 250 μm[59] and accumulate small silt particles in their gut.[60] Settled fullerene nanoparticles pack the *C. riparius* larval gut after exposure.[61] Thus, their mode of feeding may create particularly high environmental exposures for *C. riparius* larvae and other deposit feeders from settled ENMs. We posit that the nano-specific impacts observed in this study are the result of the concentration of ENMs in surface sand due to settling, with the likely mode of exposure being ingestion due to *C. riparius* deposit feeding. Whether observed impacts are the result of LCO and NMC exposure directly or the result of material dissolution in the gut or in cellular compartments such as the lysosome (where low pH would be predicted to enhance dissolution)[18] is beyond the scope of this study. Future studies using x-ray computed tomography and x-ray fluorescence techniques to determine the distribution of particles and ions in the organism[62,63] could be informative.

Bioavailability of aggregated ENMs in the benthos may depend on their interaction with sediment particles.[64] Most studies have examined interactions of ENMs with soils rather than sediments,[64] but soil studies have observed that Ag ENMs bind more tightly to clay particles than

404 to sand.[65] Thus, our use of sand as a model sediment in this study may mean that settled LCO
405 and NMC are more bioavailable than they might be in sediments with high clay content.
406
407 Impacts on *C. riparius* development and emergence observed in this study would be expected to
408 negatively impact reproductive success,[66] which could impact higher trophic levels due to their
409 position as a keystone species in aquatic and terrestrial environments.[67] ENM ingestion could
410 also result in trophic transfer of ENMs as they are a primary food resource for many fish
411 species.[68] Bioaccumulation of ENMs in chironomids has been shown for Ag and CeO_2
412 ENMs.[68,69] CeO_2 ENMs were shown to transfer from chironomids to amphibian larvae, where
413 they accumulated and caused genotoxicity.[68] Thus benthic organisms such as *C. riparius* may act
414 as important vectors for ENMs to enter the aquatic food chain, even when these particles are not
415 stable in the water column.
416
417 Modeling studies have shown that for large lakes with long residence times, upwards of 98% of
418 input ENMs can be anticipated to be retained within the lake system due to settling.[70] This means
419 that reaching the sediment concentration found to cause impacts in this study — 23 $\mu g \cdot cm^{-2}$ for
420 10 $mg \cdot L^{-1}$ exposures — would only require a detectable steady-state ENM concentration of 50
421 $ng \cdot L^{-1}$ in surface water. TiO_2 ENMs were detectable in a European lake at 1.4 $\mu g \cdot L^{-1}$.[71] No study
422 has yet been done to model or measure amounts of LCO or NMC in the environment. The most
423 likely source of LCO or NMC in the environment would be as leachate from LIB waste in
424 landfills, as LIBs are generally not recycled.[14,17] Co leached from LIBs in standard tests was
425 found to be on the order of 164,000 mg Co per kg of battery.[14] Hendren et al. have proposed that
426 production volume may be an indicator of likely exposure risk,[72] and production does correlate

427 to some degree with modeled and measured environmental concentrations of ENMs.[73] The total
428 mass of LIBs used globally in 2016 was estimated at 374,000 metric tons.[14] Depending on
429 battery life expectancy, this same mass of batteries can be expected to be discarded as waste
430 within years.[14] Given the amount of Co leached from batteries, 60,000 metric tons annually of
431 Co waste will be emitted from LIBs. In this case metal oxide battery waste will be on the same
432 order of magnitude as annual US production estimated for TiO_2 (38,000 tons).[72] Given that TiO_2
433 has been modeled[74] and measured[71] to be present in surface waters at around 1 $\mu g \cdot L^{-1}$, a
434 significant amount of LCO and NMC may be expected to be found in the environment based on
435 the expected mass of LIB waste. The 50 $ng \cdot L^{-1}$ steady-state estimate corresponding to our 10
436 $mg \cdot L^{-1}$ exposure may not be unrealistic in such a scenario.
437
438 ***Implications***
439 The expected increase in use of battery cathode materials such as LCO and NMC in the next
440 decade and the lack of material recycling means that environmental release due to disposal may
441 be expected.[16,17] Exposure to LCO and NMC caused significant impacts on the growth and
442 development of *C. riparius* through stress pathways and inhibition of heme synthesis. Settling of
443 nanomaterials creates the potential for small amounts of complex metal oxides and other ENMs
444 to accumulate in the benthos of aquatic systems at concentrations that may cause adverse
445 impacts. Reduced impact of NMC versus LCO points to tuning of material composition as a
446 means of limiting environmental effects of material release.
447
448 **Acknowledgements**

This work was supported by National Science Foundation under the Center for Sustainable Nanotechnology (CSN), CHE-1503408. The CSN is part of the Centers for Chemical Innovation Program. Gene expression work was conducted at the Great Lakes Genomics Center at UW-Milwaukee. The authors acknowledge Nicklaus Neureuther and Dylan Olson for help with culture maintenance and exposure takedowns. Thank you to the Johns Hopkins Department of Environmental Health and Engineering for use of their equipment.

Disclosure of interests

The authors declare no competing financial interest.

Supporting Information Available

Supporting Methods, Tables, and Figures.

This information is available free of charge via the Internet at http://pubs.acs.org.

References

(1) Lin, S.; Wang, H.; Yu, T. A Promising Trend for Nano-EHS Research — Integrating Fate and Transport Analysis with Safety Assessment Using Model Organisms. *NanoImpact* **2017**, *7*, 1–6. https://doi.org/10.1016/j.impact.2016.09.007.

(2) Petosa, A. R.; Jaisi, D. P.; Quevedo, I. R.; Elimelech, M.; Tufenkji, N. Aggregation and Deposition of Engineered Nanomaterials in Aquatic Environments: Role of Physicochemical Interactions. *Environ. Sci. Technol.* **2010**, *44* (17), 6532–6549. https://doi.org/10.1021/es100598h.

(3) Koelmans, A. A.; Diepens, N. J.; Velzeboer, I.; Besseling, E.; Quik, J. T. K.; van de

Meent, D. Guidance for the Prognostic Risk Assessment of Nanomaterials in Aquatic Ecosystems. *Sci. Total Environ.* **2015**, *535*, 141–149. https://doi.org/10.1016/j.scitotenv.2015.02.032.

(4) Jennings, V.; Goodhead, R.; Tyler, C. R. Ecotoxicology of Nanomaterials in Aquatic Systems. In *Characterization of Nanomaterials in Complex Environmental and Biological Media*; Baalousha, M., Lead, J. R., Eds.; Elsevier, 2015; pp 25–32.

(5) Maynard, A. D.; Warheit, D. B.; Philbert, M. A. The New Toxicology of Sophisticated Materials: Nanotoxicology and Beyond. *Toxicol. Sci.* **2011**, *120* (Supplement 1), S109–S129. https://doi.org/10.1093/toxsci/kfq372.

(6) Bondarenko, O.; Juganson, K.; Ivask, A.; Kasemets, K.; Mortimer, M.; Kahru, A. Toxicity of Ag, CuO and ZnO Nanoparticles to Selected Environmentally Relevant Test Organisms and Mammalian Cells in Vitro: A Critical Review. *Arch. Toxicol.* **2013**, *87* (7), 1181–1200. https://doi.org/10.1007/s00204-013-1079-4.

(7) Brodd, R. J. *Batteries for Sustainability : Selected Entries from the Encyclopedia of Sustainability Science and Technology*; Springer, 2012.

(8) Grey, C. P.; Ceder, G.; Kang, K.; Meng, Y. S.; Bre, J. Electrodes with High Power and High Capacity for Rechargeable Lithium Batteries. *Science.* **2005**, *311* (December), 1–5. https://doi.org/10.1126/science.1122152.

(9) Pollet, B. G.; Staffell, I.; Shang, J. L. Current Status of Hybrid, Battery and Fuel Cell Electric Vehicles: From Electrochemistry to Market Prospects. *Electrochim. Acta* **2012**, *84*, 235–249. https://doi.org/10.1016/j.electacta.2012.03.172.

(10) Wang, Y.; Yu, Y.; Huang, K.; Chen, B.; Deng, W.; Yao, Y. Quantifying the Environmental Impact of a Li-Rich High-Capacity Cathode Material in Electric Vehicles

via Life Cycle Assessment. *Environ. Sci. Pollut. Res.* **2017**, *24* (2), 1251–1260. https://doi.org/10.1007/s11356-016-7849-9.

(11) Liu, H.; Zhou, Y.; Moré, R.; Müller, R.; Fox, T.; Patzke, G. R. Correlations among Structure, Electronic Properties, and Photochemical Water Oxidation: A Case Study on Lithium Cobalt Oxides. *ACS Catal.* **2015**, *5* (6), 3791–3800. https://doi.org/10.1021/acscatal.5b00078.

(12) Hang, M. N.; Hudson-Smith, N. V.; Clement, P. L.; Zhang, Y.; Wang, C.; Haynes, C. L.; Hamers, R. J. Influence of Nanoparticle Morphology on Ion Release and Biological Impact of Nickel Manganese Cobalt Oxide (NMC) Complex Oxide Nanomaterials. *ACS Appl. Nano Mater.* **2018**, *1* (4), 1721–1730. https://doi.org/10.1021/acsanm.8b00187.

(13) Olivetti, E. A.; Ceder, G.; Gaustad, G. G.; Fu, X. Lithium-Ion Battery Supply Chain Considerations: Analysis of Potential Bottlenecks in Critical Metals. *Joule* **2017**, *1* (2), 229–243. https://doi.org/10.1016/j.joule.2017.08.019.

(14) Winslow, K. M.; Laux, S. J.; Townsend, T. G. A Review on the Growing Concern and Potential Management Strategies of Waste Lithium-Ion Batteries. *Resources, Conservation and Recycling*. Elsevier 2018, pp 263–277. https://doi.org/10.1016/j.resconrec.2017.11.001.

(15) Zou, H.; Gratz, E.; Apelian, D.; Wang, Y. A Novel Method to Recycle Mixed Cathode Materials for Lithium Ion Batteries. *Green Chem.* **2013**, *15* (5), 1183. https://doi.org/10.1039/c3gc40182k.

(16) Kang, D. H. P.; Chen, M.; Ogunseitan, O. A. Potential Environmental and Human Health Impacts of Rechargeable Lithium Batteries in Electronic Waste. *Environ. Sci. Technol.* **2013**, *47* (10), 5495–5503. https://doi.org/10.1021/es400614y.

518 (17) Hamers, R. J. Nanomaterials and Global Sustainability. *Acc. Chem. Res.* **2017**, *50* (3),
519 633–637. https://doi.org/10.1021/acs.accounts.6b00634.
520 (18) Bennett, J. W.; Jones, D.; Huang, X.; Hamers, R. J.; Mason, S. E. Dissolution of Complex
521 Metal Oxides from First-Principles and Thermodynamics: Cation Removal from the (001)
522 Surface of Li(Ni 1/3 Mn 1/3 Co 1/3)O 2. *Environ. Sci. Technol.* **2018**, *52* (10), 5792–
523 5802. https://doi.org/10.1021/acs.est.8b00054.
524 (19) Bozich, J.; Hang, M.; Hamers, R.; Klaper, R. Core Chemistry Influences the Toxicity of
525 Multicomponent Metal Oxide Nanomaterials, Lithium Nickel Manganese Cobalt Oxide,
526 and Lithium Cobalt Oxide to Daphnia Magna. *Environ. Toxicol. Chem.* **2017**, *36* (9),
527 2493–2502. https://doi.org/10.1002/etc.3791.
528 (20) Béchard, K. M.; Gillis, P. L.; Wood, C. M. Acute Toxicity of Waterborne Cd, Cu, Pb, Ni,
529 and Zn to First-Instar Chironomus Riparius Larvae. *Arch. Environ. Contam. Toxicol.*
530 **2008**, *54* (3), 454–459. https://doi.org/10.1007/s00244-007-9048-7.
531 (21) Besser, J. M.; Brumbaugh, W. G.; Ingersoll, C. G.; Ivey, C. D.; Kunz, J. L.; Kemble, N.
532 E.; Schlekat, C. E.; Garman, E. R. Chronic Toxicity of Nickel-Spiked Freshwater
533 Sediments: Variation in Toxicity among Eight Invertebrate Taxa and Eight Sediments.
534 *Environ. Toxicol. Chem.* **2013**, *32* (11), n/a-n/a. https://doi.org/10.1002/etc.2271.
535 (22) Khangarot, B. S.; Ray, P. K. Sensitivity of Midge Larvae OfChironomus Tentans
536 Fabricius (Diptera Chironomidae) to Heavy Metals. *Bull. Environ. Contam. Toxicol.* **1989**,
537 *42* (3), 325–330. https://doi.org/10.1007/BF01699956.
538 (23) Münzinger, A. Effects of Nickel on Daphnia Magna during Chronic Exposure and
539 Alterations in the Toxicity to Generations Pre-Exposed to Nickel. *Water Res.* **1990**, *24* (7),
540 845–852. https://doi.org/10.1016/0043-1354(90)90134-R.

(24) Subba Rao, D.; Saxena, A. B. Research Report: Acute Toxicity of Mercury, Zinc, Lead, Cadmium, Manganese to the Chironomus Sp. *Int. J. Environ. Stud.* **1981**, *16* (3–4), 225–226. https://doi.org/10.1080/00207238108709874.

(25) Fjällborg, B.; Li, B.; Nilsson, E.; Dave, G. Toxicity Identification Evaluation of Five Metals Performed with Two Organisms (Daphnia Magna and Lactuca Sativa). *Arch. Environ. Contam. Toxicol.* **2006**, *50* (2), 196–204. https://doi.org/10.1007/s00244-005-7017-6.

(26) Van Koetsem, F.; Verstraete, S.; Van der Meeren, P.; Du Laing, G. Stability of Engineered Nanomaterials in Complex Aqueous Matrices: Settling Behaviour of CeO2 Nanoparticles in Natural Surface Waters. *Environ. Res.* **2015**, *142*, 207–214. https://doi.org/10.1016/j.envres.2015.06.028.

(27) Zhang, Y.; Chen, Y.; Westerhoff, P.; Hristovski, K.; Crittenden, J. C. Stability of Commercial Metal Oxide Nanoparticles in Water. *Water Res.* **2008**, *42* (8–9), 2204–2212. https://doi.org/10.1016/j.watres.2007.11.036.

(28) Velzeboer, I.; Hendriks, A. J.; Ragas, A. M. J.; van de Meent, D. Aquatic Ecotoxicity Tetst of Some Nanomaterials. *Environ. Toxicol. Chem.* **2008**, *27* (9), 1942. https://doi.org/10.1897/07-509.1.

(29) Armitage, P. D.; Cranston, P. S.; Pinder, L. C. V. *The Chironomidae : Biology and Ecology of Non-Biting Midges*, 1st ed.; Chapman & Hall, 1995.

(30) Besten, P. J. den.; Munawar, M. *Ecotoxicological Testing of Marine and Freshwater Ecosystems : Emerging Techniques, Trends, and Strategies*; Taylor & Francis, 2005.

(31) Oppold, A. M.; Schmidt, H.; Rose, M.; Hellmann, S. L.; Dolze, F.; Ripp, F.; Weich, B.; Schmidt-Ott, U.; Schmidt, E.; Kofler, R.; Hankeln, T., Pfenninger, M. Chironomus

564 Riparius (Diptera) Genome Sequencing Reveals the Impact of Minisatellite Transposable
565 Elements on Population Divergence. *Mol. Ecol.* **2017**, *26* (12), 3256–3275.
566 https://doi.org/10.1111/mec.14111.
567 (32) Park, S.-Y.; Chung, J.; Colman, B. P.; Matson, C. W.; Kim, Y.; Lee, B.-C.; Kim, P.-J.;
568 Choi, K.; Choi, J. Ecotoxicity of Bare and Coated Silver Nanoparticles in the Aquatic
569 Midge, Chironomus Riparius. *Environ. Toxicol. Chem.* **2015**, *34* (9), 2023–2032.
570 https://doi.org/10.1002/etc.3019.
571 (33) Gopalakrishnan Nair, P. M.; Chung, I. M. Alteration in the Expression of Antioxidant and
572 Detoxification Genes in Chironomus Riparius Exposed to Zinc Oxide Nanoparticles.
573 *Comp. Biochem. Physiol. Part B Biochem. Mol. Biol.* **2015**, *190*, 1–7.
574 https://doi.org/10.1016/j.cbpb.2015.08.004.
575 (34) Waissi-Leinonen, G. C.; Petersen, E. J.; Pakarinen, K.; Akkanen, J.; Leppänen, M. T.;
576 Kukkonen, J. V. K. Toxicity of Fullerene (C60) to Sediment-Dwelling Invertebrate
577 Chironomus Riparius Larvae. *Environ. Toxicol. Chem.* **2012**, *31* (9), 2108–2116.
578 https://doi.org/10.1002/etc.1926.
579 (35) Nair, P. M. G.; Park, S. Y.; Lee, S.-W.; Choi, J. Differential Expression of Ribosomal
580 Protein Gene, Gonadotrophin Releasing Hormone Gene and Balbiani Ring Protein Gene
581 in Silver Nanoparticles Exposed Chironomus Riparius. *Aquat. Toxicol.* **2011**, *101* (1), 31–
582 37. https://doi.org/10.1016/j.aquatox.2010.08.013.
583 (36) Lee, S.-W.; Kim, S.-M.; Choi, J. Genotoxicity and Ecotoxicity Assays Using the
584 Freshwater Crustacean Daphnia Magna and the Larva of the Aquatic Midge Chironomus
585 Riparius to Screen the Ecological Risks of Nanoparticle Exposure. *Environ. Toxicol.*
586 *Pharmacol.* **2009**, *28* (1), 86–91. https://doi.org/10.1016/j.etap.2009.03.001.

587 (37) Doɬangün, M.; Hang, M. N.; Troiano, J. M.; McGeachy, A. C.; Melby, E. S.; Pedersen, J.
588 A.; Hamers, R. J.; Geiger, F. M. Alteration of Membrane Compositional Asymmetry by
589 LiCoO<inf>2</Inf> Nanosheets. *ACS Nano* **2015**, *9* (9), 8755–8765.
590 https://doi.org/10.1021/acsnano.5b01440.
591 (38) Hang, M. N.; Gunsolus, I. L.; Wayland, H.; Melby, E. S.; Mensch, A. C.; Hurley, K. R.;
592 Pedersen, J. A.; Haynes, C. L.; Hamers, R. J. Impact of Nanoscale Lithium Nickel
593 Manganese Cobalt Oxide (NMC) on the Bacterium *Shewanella Oneidensis* MR-1. *Chem.*
594 *Mater.* **2016**, *28* (4), 1092–1100. https://doi.org/10.1021/acs.chemmater.5b04505.
595 (39) Livak, K. J.; Schmittgen, T. D. Analysis of Relative Gene Expression Data Using Real-
596 Time Quantitative PCR and the 2−ΔΔCT Method. *Methods* **2001**, *25* (4), 402–408.
597 https://doi.org/10.1006/meth.2001.1262.
598 (40) Markus, A. A.; Parsons, J. R.; Roex, E. W. M.; de Voogt, P.; Laane, R. W. P. M.
599 Modeling Aggregation and Sedimentation of Nanoparticles in the Aquatic Environment.
600 *Sci. Total Environ.* **2015**, *506–507*, 323–329.
601 https://doi.org/10.1016/J.SCITOTENV.2014.11.056.
602 (41) Brunelli, A.; Pojana, G.; Callegaro, S.; Marcomini, A. Agglomeration and Sedimentation
603 of Titanium Dioxide Nanoparticles (n-TiO2) in Synthetic and Real Waters. *J.*
604 *Nanoparticle Res.* **2013**, *15* (6), 1684. https://doi.org/10.1007/s11051-013-1684-4.
605 (42) Baalousha, M. Aggregation and Disaggregation of Iron Oxide Nanoparticles: Influence of
606 Particle Concentration, PH and Natural Organic Matter. *Sci. Total Environ.* **2009**, *407* (6),
607 2093–2101. https://doi.org/10.1016/J.SCITOTENV.2008.11.022.
608 (43) Baalousha, M. Effect of Nanomaterial and Media Physicochemical Properties on
609 Nanomaterial Aggregation Kinetics. *NanoImpact* **2017**, *6*, 55–68.

https://doi.org/10.1016/J.IMPACT.2016.10.005.

(44) Milani, D.; Reynoldson, T. B.; Borgmann, U.; Kolasa, J. The Relative Sensitivity of Four Benthic Invertebrates to Metals in Spiked-Sediment Exposures and Application to Contaminated Field Sediment. In *Environmental Toxicology and Chemistry*; John Wiley & Sons, Ltd, 2003; Vol. 22, pp 845–854. https://doi.org/10.1897/1551-5028(2003)022<0845:TRSOFB>2.0.CO;2.

(45) Thorgersen, M. P.; Downs, D. M. Cobalt Targets Multiple Metabolic Processes in Salmonella Enterica. *J. Bacteriol.* **2007**, *189* (21), 7774–7781. https://doi.org/10.1128/JB.00962-07.

(46) Misra, M.; Rodriguez, R. E.; Kasprzak, K. S. Nickel Induced Lipid Peroxidation in the Rat: Correlation with Nickel Effect on Antioxidant Defense Systems. *Toxicology* **1990**, *64* (1), 1–17. https://doi.org/10.1016/0300-483X(90)90095-X.

(47) Alarifi, S.; Ali, D.; Y, A. O. S.; Ahamed, M.; Siddiqui, M. A.; Al-Khedhairy, A. A. Oxidative Stress Contributes to Cobalt Oxide Nanoparticles-Induced Cytotoxicity and DNA Damage in Human Hepatocarcinoma Cells. *Int. J. Nanomedicine* **2013**, *8*, 189–199. https://doi.org/10.2147/IJN.S37924.

(48) Ahamed, M.; Ali, D.; Alhadlaq, H. A.; Akhtar, M. J. Nickel Oxide Nanoparticles Exert Cytotoxicity via Oxidative Stress and Induce Apoptotic Response in Human Liver Cells (HepG2). *Chemosphere* **2013**, *93* (10), 2514–2522. https://doi.org/10.1016/j.chemosphere.2013.09.047.

(49) Casalino, E.; Calzaretti, G.; Sblano, C.; Landriscina, C. Molecular Inhibitory Mechanisms of Antioxidant Enzymes in Rat Liver and Kidney by Cadmium. *Toxicology* **2002**, *179* (1–2), 37–50. https://doi.org/10.1016/S0300-483X(02)00245-7.

633 (50) Covaliu, C. I.; Matei, C.; Litescu, S.; Eremia, S. A.-M.; Stanica, N.; Diamandescu, L.;
634 Ianculescu, A.; Jitaru, I.; Berger, D. Radical Scavenger Properties of Oxide Nanoparticles
635 Stabilized with Biopolymer Matrix. *Mater. Plast.* **2010**, *47* (1).
636 (51) Kim, B. M.; Choi, B. S.; Lee, K. W.; Ki, J. S.; Kim, I. C.; Choi, I. Y.; Rhee, J. S.; Lee, J.
637 S. Expression Profile Analysis of Antioxidative Stress and Developmental Pathway Genes
638 in the Manganese-Exposed Intertidal Copepod Tigriopus Japonicus with 6K Oligochip.
639 *Chemosphere* **2013**, *92* (9), 1214–1223.
640 https://doi.org/10.1016/j.chemosphere.2013.04.047.
641 (52) Maines, M. D. Evidence for the Catabolism of Polychlorinated Biphenyl-Induced
642 Cytochrome P-448 by Microsomal Heme Oxygenase, and the Inhibition of Delta-
643 Aminolevulinate Dehydratase by Polychlorinated Biphenyls. *J. Exp. Med.* **1976**, *144* (6),
644 1509–1519.
645 (53) Maines, M. D.; Sinclair, P. Cobalt Regulation of Heme Synthesis and Degradation in
646 Avian Embryo Liver Cell Culture. *J. Biol. Chem.* **1977**, *252* (1), 219–223.
647 (54) Ranquet, C.; Ollagnier-de-Choudens, S.; Loiseau, L.; Barras, F.; Fontecave, M. Cobalt
648 Stress in Escherichia Coli. The Effect on the Iron-Sulfur Proteins. *J. Biol. Chem.* **2007**,
649 *282* (42), 30442–30451. https://doi.org/10.1074/jbc.M702519200.
650 (55) Yasukochi, Y.; Nakamura, M.; Minakami, S. Effect of Cobalt on the Synthesis and
651 Degradation of Hepatic Catalase in Vivo. *Biochem. J.* **1974**, *144* (3), 455–464.
652 (56) Kubrak, O. I.; Husak, V. V.; Rovenko, B. M.; Storey, J. M.; Storey, K. B.; Lushchak, V. I.
653 Cobalt-Induced Oxidative Stress in Brain, Liver and Kidney of Goldfish Carassius
654 Auratus. *Chemosphere* **2011**, *85* (6), 983–989.
655 https://doi.org/10.1016/j.chemosphere.2011.06.078.

(57) Walshe, B. Y. B. M. THE FUNCTION OF HAEMOGLOBIN IN TANYTARSUS (CHIRONOMIDAE). *J. Exp. Biol.* **1947**, *24* (3–4), 343–351.

(58) Peijnenburg, W. J. G. M.; Baalousha, M.; Chen, J.; Chaudry, Q.; Von Der Kammer, F.; Kuhlbusch, T. A. J.; Lead, J.; Nickel, C.; Quik, J. T. K.; Renker, M.; et al. A Review of the Properties and Processes Determining the Fate of Engineered Nanomaterials in the Aquatic Environment. *Crit. Rev. Environ. Sci. Technol.* **2015**, *45* (19), 2084–2134. https://doi.org/10.1080/10643389.2015.1010430.

(59) Ptatscheck, C.; Putzki, H.; Traunspurger, W. Impact of Deposit-Feeding Chironomid Larvae (*Chironomus Riparius*) on Meiofauna and Protozoans. *Freshw. Sci.* **2017**, *36* (4), 796–804. https://doi.org/10.1086/694461.

(60) Rasmussen, J. B. Comparison of Gut Contents and Assimilation Efficiency of Fourth Instar Larvae of Two Coexisting Chironomids, *Chironomus Riparius* Meigen and *Glyptotendipes Paripes* (Edwards). *Can. J. Zool.* **1984**, *62* (6), 1022–1026. https://doi.org/10.1139/z84-145.

(61) Waissi, G. C.; Bold, S.; Pakarinen, K.; Akkanen, J.; Leppänen, M. T.; Petersen, E. J.; Kukkonen, J. V. K. Chironomus Riparius Exposure to Fullerene-Contaminated Sediment Results in Oxidative Stress and May Impact Life Cycle Parameters. *J. Hazard. Mater.* **2017**, *322*, 301–309. https://doi.org/10.1016/j.jhazmat.2016.04.015.

(62) Chaurand, P.; Liu, W.; Borschneck, D.; Levard, C.; Auffan, M.; Paul, E.; Collin, B.; Kieffer, I.; Lanone, S.; Rose, J.; et al. Multi-Scale X-Ray Computed Tomography to Detect and Localize Metal-Based Nanomaterials in Lung Tissues of in Vivo Exposed Mice. *Sci. Rep.* **2018**, *8* (1), 4408. https://doi.org/10.1038/s41598-018-21862-4.

(63) Cagno, S.; Brede, D. A.; Nuyts, G.; Vanmeert, F.; Pacureanu, A.; Tucoulou, R.; Cloetens,

679 P.; Falkenberg, G.; Janssens, K.; Salbu, B.; et al. Combined Computed Nanotomography
680 and Nanoscopic X-Ray Fluorescence Imaging of Cobalt Nanoparticles in *Caenorhabditis*
681 *Elegans*. *Anal. Chem.* **2017**, *89* (21), 11435–11442.
682 https://doi.org/10.1021/acs.analchem.7b02554.
683 (64) Cross, R. K.; Tyler, C.; Galloway, T. S. Transformations That Affect Fate, Form and
684 Bioavailability of Inorganic Nanoparticles in Aquatic Sediments. *Environ. Chem.* **2015**, *12*
685 (6), 627. https://doi.org/10.1071/EN14273.
686 (65) Cornelis, G.; Pang, L.; Doolette, C.; Kirby, J. K.; McLaughlin, M. J. Transport of Silver
687 Nanoparticles in Saturated Columns of Natural Soils. *Sci. Total Environ.* **2013**, *463–464*,
688 120–130. https://doi.org/10.1016/J.SCITOTENV.2013.05.089.
689 (66) Péry, A. R. R.; Mons, R.; Flammarion, P.; Lagadic, L.; Garric, J. A Modeling Approach to
690 Link Food Availability, Growth, Emergence, and Reproduction for the Midge
691 *Chironomus Riparius*. *Environ. Toxicol. Chem.* **2002**, *21* (11), 2507–2513.
692 https://doi.org/10.1002/etc.5620211133.
693 (67) Azevedo-Pereira, H. M. V. S.; Soares, A. M. V. M. Effects of Mercury on Growth,
694 Emergence, and Behavior of Chironomus Riparius Meigen (Diptera: Chironomidae).
695 *Arch. Environ. Contam. Toxicol.* **2010**, *59* (2), 216–224. https://doi.org/10.1007/s00244-
696 010-9482-9.
697 (68) Bour, A.; Mouchet, F.; Cadarsi, S.; Silvestre, J.; Baqué, D.; Gauthier, L.; Pinelli, E. CeO2
698 Nanoparticle Fate in Environmental Conditions and Toxicity on a Freshwater Predator
699 Species: A Microcosm Study. *Environ. Sci. Pollut. Res.* **2017**, *24* (20), 17081–17089.
700 https://doi.org/10.1007/s11356-017-9346-1.
701 (69) Lowry, G. V.; Espinasse, B. P.; Badireddy, A. R.; Richardson, C. J.; Reinsch, B. C.;

Bryant, L. D.; Bone, A. J.; Deonarine, A.; Chae, S.; Therezien, M.; et al. Long-Term Transformation and Fate of Manufactured Ag Nanoparticles in a Simulated Large Scale Freshwater Emergent Wetland. *Environ. Sci. Technol.* **2012**, *46* (13), 7027–7036. https://doi.org/10.1021/es204608d.

(70) Koelmans, A. A.; Quik, J. T. K.; Velzeboer, I. Lake Retention of Manufactured Nanoparticles. *Environ. Pollut.* **2015**, *196*, 171–175. https://doi.org/10.1016/j.envpol.2014.09.025.

(71) Gondikas, A. P.; Kammer, F. von der; Reed, R. B.; Wagner, S.; Ranville, J. F.; Hofmann, T. Release of TiO2 Nanoparticles from Sunscreens into Surface Waters: A One-Year Survey at the Old Danube Recreational Lake. *Environ. Sci. Technol.* **2014**, *48* (10), 5415–5422. https://doi.org/10.1021/es405596y.

(72) Hendren, C. O.; Mesnard, X.; Dröge, J.; Wiesner, M. R. Estimating Production Data for Five Engineered Nanomaterials as a Basis for Exposure Assessment. *Environ. Sci. Technol.* **2011**, *45* (7), 2562–2569. https://doi.org/10.1021/es103300g.

(73) Gottschalk, F.; Sun, T.; Nowack, B. Environmental Concentrations of Engineered Nanomaterials: Review of Modeling and Analytical Studies. *Environ. Pollut.* **2013**, *181*, 287–300. https://doi.org/10.1016/j.envpol.2013.06.003.

(74) Gottschalk, F.; Sun, T.; Nowack, B. Environmental Concentrations of Engineered Nanomaterials: Review of Modeling and Analytical Studies. *Environ. Pollut.* **2013**, *181*, 287–300. https://doi.org/10.1016/j.envpol.2013.06.003.

Figures

Figure 1. Differences in *C. riparius* larval size and Hb after 7 d exposure

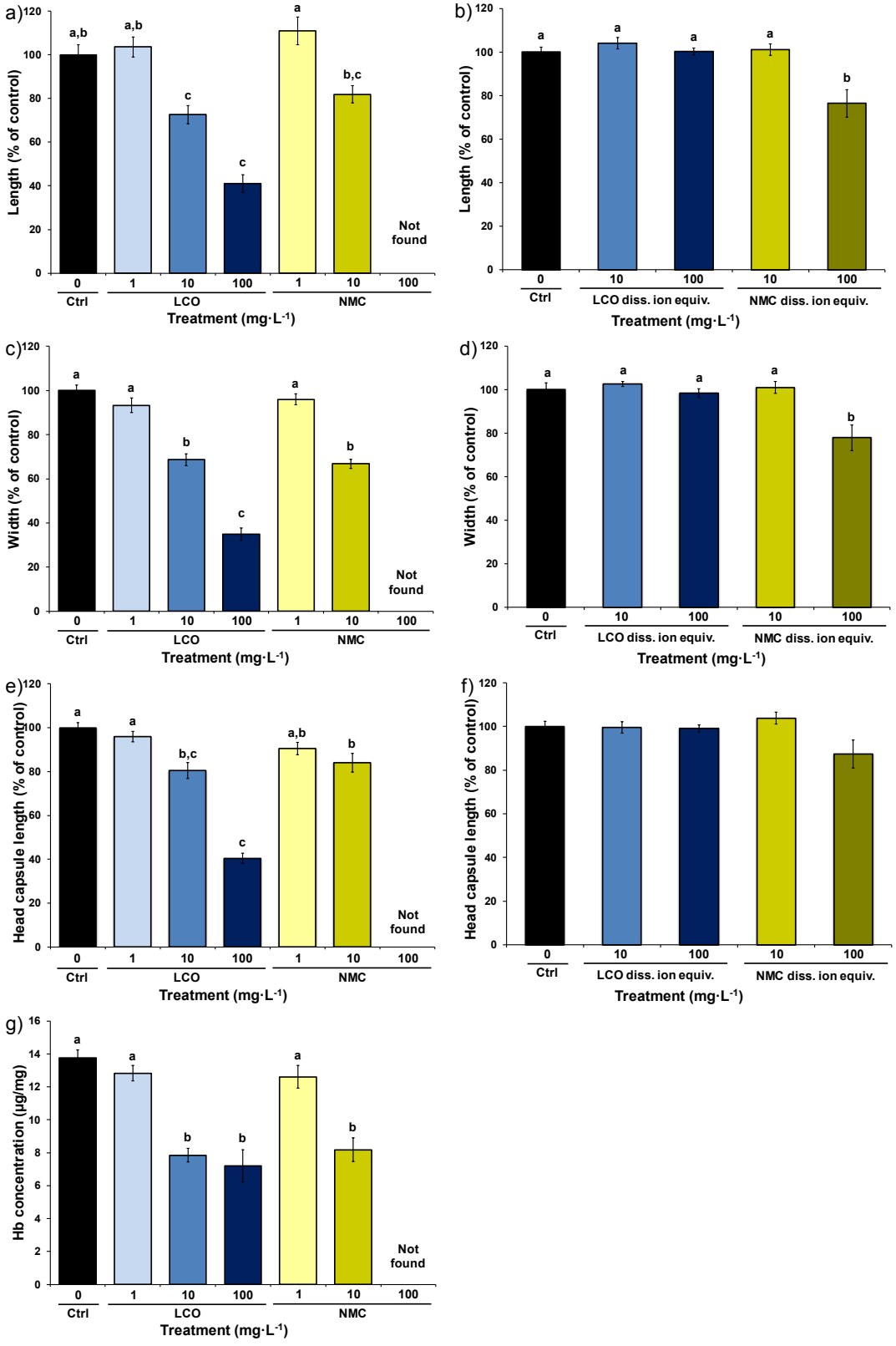

Figure 2. Differences in *C. riparius* time to emergence as adult flies

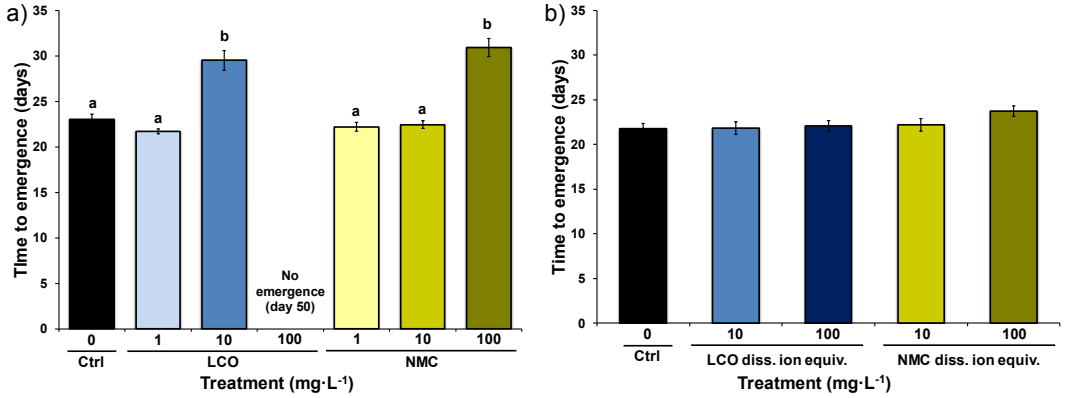

749 **Figure 3. Differences in *C. riparius* larval gene expression after 7 day exposure**

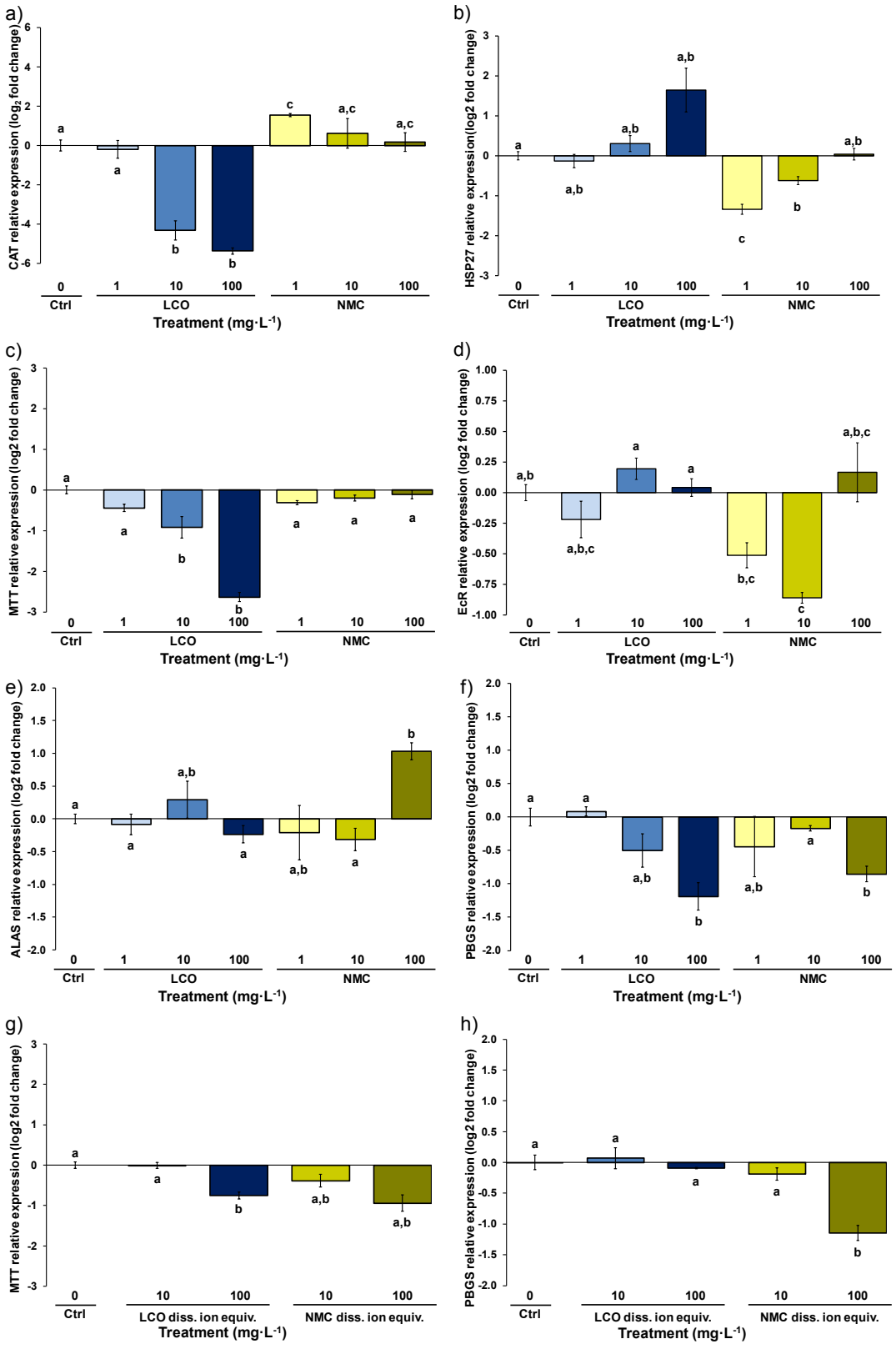

750

751

752

753

Figure 4. Proposed adverse outcome pathway for *C. riparius* LCO and NMC exposure

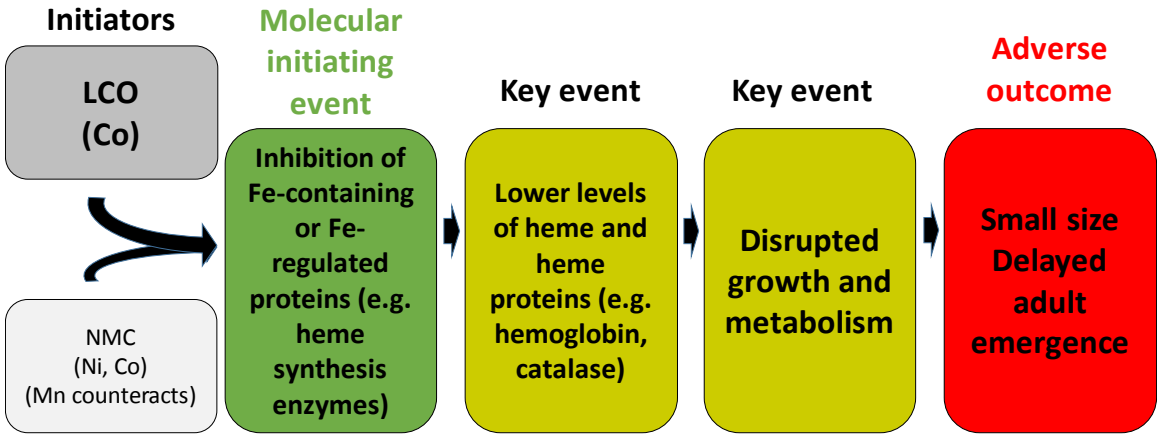

Figure legends

Figure 1. Differences in *C. riparius* larval size and Hb after 7 d exposure. LCO and NMC particle exposure induces significant impacts on larval size and Hb levels on exposure day 7. Size data (percent of control) for particle and ion exposed larvae. a) Particle-exposed larvae lengths, b) ion-exposed larvae lengths, c) particle-exposed larvae width, d) ion-exposed larvae width, e) particle-exposed larvae head capsule length, f) ion-exposed larvae head capsule length. Columns with different letters differ significantly ($p < 0.05$) by Kruskal-Wallis (panels a, b, e, f) or one-way nested ANOVA with Tukey post-hoc tests (panels c and d). g) Hb concentration calculated from green absorbance for all larvae harvested a day 7. Columns with different letters indicate a significant difference ($p < 0.05$) by one-way nested ANOVA with Tukey post-hoc tests. Error bars represent SEM.

Figure 2. Differences in *C. riparius* time to emergence as adult flies. Time to emergence for a) control and LCO and NMC particle-exposed and b) control and LCO and NMC ion exposed

772 animals. Columns with different letters differ significantly ($p < 0.05$) by Kaplan-Meier non-
773 parametric analysis. Error bars represent SEM.
774
775 **Figure 3. Differences in *C. riparius* larval gene expression after 7 d exposure.** Log_2 fold
776 change values for LCO and NMC particle-exposed larvae harvested at day 7. Results are shown
777 for a) *CAT*, b) *HSP27*, c) *MTT*, d) *EcR*, e) *ALAS*, and f) *PBGS*. Results for ion-exposed animals
778 are also shown for g) *MTT* and h) *PBGS*. Columns with different letters differ significantly ($p <$
779 0.05) by one-way Welch ANOVA with Dunnett's T3 post-hoc comparisons. Error bars represent
780 SEM.
781
782 **Figure 4. Proposed adverse outcome pathway for *C. riparius* LCO and NMC exposure.** A
783 proposed adverse outcome pathway for *C. riparius* larval exposure to LCO and NMC showing
784 inhibition of iron-containing or iron-regulated proteins by cobalt as the molecular initiating
785 event, resulting in lowered levels of heme and heme proteins, which in turn causes disruption to
786 normal growth and metabolism, culminating in the adverse outcome of smaller size and delayed
787 emergence as adult flies.